Two-Photon Absorption Cross-Sections from Electronic Structure Methods: Mesoionic Compounds

Gustavo L. C. Moura and Alfredo M. Simas*

Departamento de Química Fundamental, CCEN, Universidade Federal de Pernambuco, 50590-470, Recife, Pernambuco, Brazil

Received February 6, 2007. Revised Manuscript Received March 14, 2008

Absorption of two photons by organic molecules has many important technological applications, making theoretical modeling and synthesis of new molecules with large values of cross-sections, $\delta(\omega)$, much needed activities. In this article, we present a computational procedure based on semiempirical electronic structure methods, which allows us to rank a series of homologous compounds in terms of $\delta(\omega)$, as well as estimate single- and two-photon absorption wavelengths. This procedure uses a truncated version of the expression for the two-photon absorption peak, which retains only 4 of the 24 terms of the nontruncated equation and results in two-photon absorption peaks that are nearly identical to the ones obtained using all 24 terms, provided the incident photon energy is far from one-photon resonances. When the incident photon energy gets closer to one-photon resonances, the negative component of the hyperpolarizability becomes dominant and we advance a simplified, but still exact, form of this negative component. We also show how to include a semiexact correction due to this negative component to the three-level approximation usually employed in the interpretation of the two-photon absorption spectra. In the calculations, we employ configuration interaction with single excitations only and argue that this INDO/S CIS approach is capable of ranking a series of homologous compounds in terms of $\delta(\omega)$. Finally, we apply this procedure to the combinatorial design of new organic compounds with quadrupolar arrangements made of two type A mesoionic rings connected through a polyenic bridge with the purpose of arriving at synthetic targets with potential for displaying large values of $\delta(\omega)$ and well-separated single- and two-photon absorption wavelengths.

1. Introduction

In two-photon absorption (TPA) processes, the energies of two photons combine to produce a single electronic excitation. The possibility of occurrence of this process was predicted theoretically by Maria Göppert-Mayer in 1931.[1] The first article detailing an experimental observation of the TPA process appeared only in 1961,[2] after the appearance of the laser. This article, together with the first observation of optical second-harmonic generation (SHG) in that same year,[3] signaled the birth of the field of nonlinear optics. Different from the SHG process, which demands materials without inversion symmetry, the TPA process does not require any symmetry conditions to occur. However, in materials with inversion symmetry, the TPA process has selection rules that differ from those of the more usual single-photon absorption. While absorption of one photon can only happen between states of different parities, absorption of two photons may only happen between states of the same parity. Thus, if inversion symmetry is extant, one- and two-photon absorptions access different excited states.

Absorption of two photons by organic molecules finds applications in areas such as 3D microfabrication,[4–8] optical data storage,[5,9–11] optical limiters,[12–16] photodynamic therapy,[17–19] and fluorescence microscopy.[20–25] Recently, absorption of

* To whom correspondence should be addressed. E-mail: simas@ufpe.br.

(1) Göppert-Mayer, M. *Ann. Phys.* **1931**, *9*, 273.
(2) Kaiser, W.; Garrett, C. G. B. *Phys. Rev. Lett.* **1961**, *7*, 229.
(3) Franken, P. A.; Weinreich, G.; Peters, C. W.; Hill, A. E. *Phys. Rev. Lett.* **1961**, *7*, 118.
(4) Maruo, S.; Nakamura, O.; Kawata, S. *Opt. Lett.* **1997**, *22*, 132.
(5) Cumpston, B. H.; Ananthavel, S. P.; Barlow, S.; Dyer, D. L.; Ehrlich, J. E.; Erskine, L. L.; Heikal, A. A.; Kuebler, S. M.; Lee, I. Y. S.; Cord-Maughon, D.; Qin, J. Q.; Rockel, H.; Rumi, M.; Wu, X. L.; Marder, S. R.; Perry, J. W. *Nature* **1999**, *398*, 51.
(6) Sun, H. B.; Matsuo, S.; Misawa, H. *Appl. Phys. Lett.* **1999**, *74*, 786.
(7) Kawata, S.; Sun, H. B.; Tanaka, T.; Takada, K. *Nature* **2001**, *412*, 697.
(8) Zhou, W. H.; Kuebler, S. M.; Braun, K. L.; Yu, T. Y.; Cammack, J. K.; Ober, C. K.; Perry, J. W.; Marder, S. R. *Science* **2002**, *296*, 1106.
(9) Pudavar, H. E.; Joshi, M. P.; Prasad, P. N.; Reinhardt, B. A. *Appl. Phys. Lett.* **1999**, *74*, 1338.
(10) Parthenopoulos, D. A.; Rentzepis, P. M. *Science* **1989**, *245*, 843.
(11) Strickler, J. H.; Webb, W. W. *Opt. Lett.* **1991**, *16*, 1780.
(12) Perry, J. W.; Mansour, K.; Lee, I. Y. S.; Wu, X. L.; Bedworth, P. V.; Chen, C. T.; Ng, D.; Marder, S. R.; Miles, P.; Wada, T.; Tian, M.; Sasabe, H. *Science* **1996**, *273*, 1533.
(13) Ehrlich, J. E.; Wu, X. L.; Lee, I. Y. S.; Hu, Z. Y.; Rockel, H.; Marder, S. R.; Perry, J. W. *Opt. Lett.* **1997**, *22*, 1843.
(14) Spangler, C. W. *J. Mater. Chem.* **1999**, *9*, 2013.
(15) He, G. S.; Xu, G. C.; Prasad, P. N.; Reinhardt, B. A.; Bhatt, J. C.; Dillard, A. G. *Opt. Lett.* **1995**, *20*, 435.
(16) Tutt, L. W.; Boggess, T. F. *Prog. Quantum Electron.* **1993**, *17*, 299.
(17) Fisher, A. M. R.; Murphree, A. L.; Gomer, C. J. *Lasers Surg. Med.* **1995**, *17*, 2.
(18) Fisher, W. G.; Partridge, W. P.; Dees, C.; Wachter, E. A. *Photochem. Photobiol.* **1997**, *66*, 141.
(19) Bhawalkar, J. D.; Kumar, N. D.; Zhao, C. F.; Prasad, P. N. *J. Clin. Laser Med. Surg.* **1997**, *15*, 201.
(20) Denk, W.; Strickler, J. H.; Webb, W. W. *Science* **1990**, *248*, 73.
(21) Konig, K. *J. Microsc.* **2000**, *200*, 83.
(22) Miller, M. J.; Wei, S. H.; Parker, I.; Cahalan, M. D. *Science* **2002**, *296*, 1869.
(23) Xu, C.; Zipfel, W.; Shear, J. B.; Williams, R. M.; Webb, W. W. *Proc. Natl. Acad. Sci. U.S.A.* **1996**, *93*, 10763.

10.1021/cm070369o CCC: $40.75
Published on Web 05/29/2008

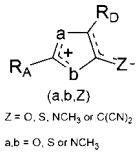

Figure 1. Molecular structure of type A mesoionic compounds,[48] represented in the present article by (*a*,*b*,*Z*), where *a* and *b* stand for the atomic symbols of the ring and *Z* for the exocyclic substituting atoms or groups.

two photons by organic molecules has also found applications in the development of sensors for metals,[26–28] fluoride anions,[29] or pH[30] for use in biological medium. These applications rely on the dependence of the probability of absorption of two photons on the square of the intensity of the incident laser, resulting in a greater spatial resolution for the process. They also rely on the fact that the photons being used possess wavelengths where absorption of one photon by the material is very weak, guaranteeing a greater penetration of the incident laser beam. Theoretical modeling and synthesis of new organic materials with large cross-sections for two-photon absorption processes, $\delta(\omega)$, are, then, much needed endeavors.

The most commonly used organic molecules for two-photon absorption applications are the ones possessing linear symmetric quadrupolar arrangements of the type donor−bridge−donor ($D-B-D$) or acceptor−bridge−acceptor ($A-B-A$).[31–37] Upon excitation, these systems exhibit charge transfer from the extremities to the center of the molecule or vice versa. In two recent papers,[38,39] Kuzyk studied the maximum fundamental limits that $\delta(\omega)$ could reach. He derived an equation that enabled him to predict the maximum possible theoretical value of $\delta(\omega)$ given the excitation energies for the first two excited states and the effective number of π electrons in the molecule. He tested his model using experimental values for a series of quadrupolar organic molecules and found that, for all the systems analyzed, the values of $\delta(\omega)$ are, at least, 2 orders of magnitude smaller than the fundamental limits. This means that there is still much potential left for developing new systems with very large values of $\delta(\omega)$. In the present paper, we investigate such possibilities.

Recently, Fujita et al. proposed[40,41] that introduction of positively charged defects in the structure of a molecule increases, by a large amount, the value of $\delta(\omega)$. They originally attributed this effect to the decrease of the excitation energy as well as the increase in the magnitude of the transition dipole moment between the ground state and the first single-photon-allowed excited state of the molecule. When this strategy was applied to the design of more realistic systems, Kishi et al. began to attribute[42,43] the increase of $\delta(\omega)$ in cationic systems to the increase in the transition dipole moment between the one-photon-allowed and two-photon-allowed excited states. Kawamata et al.[44] observed this proposed cationic effect experimentally.

All of the neutral molecules already studied as systems with large values of $\delta(\omega)$ have in common the fact that they are able to be represented by structures with covalent bonds without the need for separation of negative and positive charges. The mesomeric betaines are neutral conjugated organic molecules that can only be represented properly by dipolar structures with the positive and negative charges delocalized within the π electron system.[45] For our studies, we chose to work with the heterocyclic mesomeric betaines. More specifically, we expect that the intrinsic charge separation in type A mesoionic compounds[46,47] will lead to molecules with large values of $\delta(\omega)$. Mesoionic compounds are members of the class of conjugated heterocyclic mesomeric betaines, isoconjugate with even nonalternant hydrocarbon dianions.[45] In 1996, we advanced the concept[48] that in type A mesoionic compounds the π electrons are delocalized over two regions separated by what are essentially two single bonds. The region that includes the exocyclic group is associated with the HOMO and a negative π charge, while the other region is associated with the LUMO and a positive π charge.[49,50] In Figure 1, we present the electronic structure of type A mesoionic compounds.

We already studied the feasibility of molecules containing type A mesoionic rings as candidates for systems with large

(24) Zipfel, W. R.; Williams, R. M.; Webb, W. W. *Nat. Biotechnol.* **2003**, *21*, 1369.
(25) Denk, W.; Svoboda, K. *Neuron* **1997**, *18*, 351.
(26) Ahn, H. C.; Yang, S. K.; Kim, H. M.; Li, S. J.; Jeon, S. J.; Cho, B. R. *Chem. Phys. Lett.* **2005**, *410*, 312.
(27) Kim, H. M.; Jeong, M. Y.; Ahn, H. C.; Jeon, S. J.; Cho, B. R. *J. Org. Chem.* **2004**, *69*, 5749.
(28) Pond, S. J. K.; Tsutsumi, O.; Rumi, M.; Kwon, O.; Zojer, E.; Bredas, J. L.; Marder, S. R.; Perry, J. W. *J. Am. Chem. Soc.* **2004**, *126*, 9291.
(29) Liu, Z. Q.; Shi, M.; Li, F. Y.; Fang, Q.; Chen, Z. H.; Yi, T.; Huang, C. H. *Org. Lett.* **2005**, *7*, 5481.
(30) Werts, M. H. V.; Gmouh, S.; Mongin, O.; Pons, T.; Blanchard-Desce, M. *J. Am. Chem. Soc.* **2004**, *126*, 16294.
(31) Albota, M.; Beljonne, D.; Bredas, J. L.; Ehrlich, J. E.; Fu, J. Y.; Heikal, A. A.; Hess, S. E.; Kogej, T.; Levin, M. D.; Marder, S. R.; Cord-Maughon, D.; Perry, J. W.; Rockel, H.; Rumi, M.; Subramaniam, C.; Webb, W. W.; Wu, X. L.; Xu, C. *Science* **1998**, *281*, 1653.
(32) Rumi, M.; Ehrlich, J. E.; Heikal, A. A.; Perry, J. W.; Barlow, S.; Hu, Z. Y.; Cord-Maughon, D.; Parker, T. C.; Rockel, H.; Thayumanavan, S.; Marder, S. R.; Beljonne, D.; Bredas, J. L. *J. Am. Chem. Soc.* **2000**, *122*, 9500.
(33) Ventelon, L.; Moreaux, L.; Mertz, J.; Blanchard-Desce, M. *Chem. Commun.* **1999**, 2055.
(34) Zojer, E.; Beljonne, D.; Kogej, T.; Vogel, H.; Marder, S. R.; Perry, J. W.; Bredas, J. L. *J. Chem. Phys.* **2002**, *116*, 3646.
(35) Zojer, E.; Beljonne, D.; Pacher, P.; Bredas, J. L. *Chem.-Eur. J.* **2004**, *10*, 2668.
(36) Wang, C. K.; Macak, P.; Luo, Y.; Agren, H. *J. Chem. Phys.* **2001**, *114*, 9813.
(37) Ventelon, L.; Moreaux, L.; Mertz, J.; Blanchard-Desce, M. *Synth. Met.* **2002**, *127*, 17.
(38) Kuzyk, M. G. *J. Chem. Phys.* **2003**, *119*, 8327.
(39) Moreno, J. P.; Kuzyk, M. G. *J. Chem. Phys.* **2005**, *123*, 194101.
(40) Fujita, H.; Nakano, M.; Takahata, M.; Yamaguchi, K. *Chem. Phys. Lett.* **2002**, *358*, 435.
(41) Fujita, H.; Nakano, M.; Takahata, M.; Yamaguchi, K. *Synth. Met.* **2003**, *137*, 1391.
(42) Kishi, R.; Nakano, M.; Yamada, S.; Kamada, K.; Ohta, K.; Nitta, T.; Yamaguchi, K. *Chem. Phys. Lett.* **2004**, *393*, 437.
(43) Kishi, R.; Nakano, M.; Yamada, S.; Kamada, K.; Ohta, K.; Nitta, T.; Yamaguchi, K. *Synth. Met.* **2005**, *154*, 181.
(44) Kawamata, J.; Akiba, M.; Tani, T.; Harada, A.; Inagaki, Y. *Chem. Lett.* **2004**, *33*, 448.
(45) Ollis, W. D.; Stanforth, S. P.; Ramsden, C. A. *Tetrahedron* **1985**, *41*, 2239.
(46) Newton, C. G.; Ramsden, C. A. *Tetrahedron* **1982**, *38*, 2965.
(47) Ramsden, C. A. *Compr. Org. Chem.* **1979**, *4*, 1171.
(48) Deoliveira, M. B.; Miller, J.; Pereira, A. B.; Galembeck, S. E.; Demoura, G. L. C.; Simas, A. M. *Phosphorus Sulfur Silicon Relat. Elem.* **1996**, *108*, 75.
(49) Moura, G. L. C. Masters Thesis, Federal University of Pernambuco: Brazil, 1996.
(50) Simas, A. M.; Miller, J.; de Athayde, P. F. *Can. J. Chem.-Rev. Can. Chim.* **1998**, *76*, 869.

second-order nonlinear optical properties.[51] More specifically, we employed semiempirical electronic structure methods to calculate the static first hyperpolarizability, $\beta(0)$, of systems containing such rings. The results were very promising. Recently, Kuzyk et al. proposed that conjugated bridges with sites of reduced conjugation may be the best paradigm for making molecules with very large values of $\beta(0)$.[52,53] We would like to add that the molecular design involving mesoionic rings that we proposed in 1996[51] can be considered as an early example of this strategy. Recently, it has been demonstrated that molecules containing type A mesoionic rings as asymmetric bridges between a donor and an acceptor groups have values of $\beta(0)$ equivalent to those of systems containing symmetric polyenic bridges containing more than seven double bonds.[54] There are already in the literature articles dealing with experimental studies of nonlinear absorptions by molecules containing type A mesoionic rings with dipolar arrangements of the type donor−mesoionic−acceptor.[55–61]

In this work, we employ semiempirical electronic structure methods to obtain values of $\delta(\omega)$ for organic molecules containing mesoionic rings. The semiempirical methods appeared as alternatives to performing electronic structure calculations for systems ordinarily inaccessible by the more demanding ab initio methods. Nowadays, semiempirical methods are applied to tasks such as (i) calculation of large numbers of molecules, as in the design of drugs or the study of nonlinear optical properties of organic molecules, (ii) repetitive calculation of a single molecular system, as in molecular dynamics or Monte Carlo simulations, and (iii) calculations of giant molecules, such as proteins or DNA.

In section 2, we describe how we obtain the cross-sections for the absorption of two photons using semiempirical electronic structure methods. In section 3, we validate our computational procedure by comparing our calculated values with experimental results, and in section 4, we present and discuss the results of our calculations obtained for organic molecules containing mesoionic rings. Finally, in section 5, we discuss the main conclusions of this work.

2. Computational Procedure

Absorption of two photons is a nonlinear optical process proportional to the imaginary part of the second dynamic hyperpolarizability of the molecule, Im $\langle\gamma(-\omega;\omega,\omega,-\omega)\rangle$. The cross-section for the absorption of two photons of frequency ω is given by

$$\delta(\omega) = \frac{4\pi^2\hbar\omega^2}{n^2c^2}L^4\mathrm{Im}\langle\gamma(-\omega;\omega,\omega,-\omega)\rangle \qquad (1)$$

where n is the refractive index of the medium, c is the speed of light, and L is a local field factor. In our calculations, we considered the systems in vacuum; therefore, both n and L are equal to 1. Experimental results measure the spherical average of $\delta(\omega)$, which can be obtained from the spherical average of γ used in eq 1 and is given by

$$\langle\gamma\rangle = \frac{1}{5}\left[\sum_i \gamma_{iiii} + \frac{1}{3}\sum_{j\neq i}(\gamma_{iijj} + \gamma_{ijij} + \gamma_{ijji})\right] \qquad (2)$$

where $i,j = x,y,z$.

The Cartesian components γ_{ijkl} are given by a sum over states (SOS) equation originally proposed by Orr and Ward in eq 43c of their article.[62] This equation was derived using time-dependent perturbation theory within the electric dipole approximation for the interaction between the molecule and the electric field of the incident laser and can be written as a sum of two parts: $\gamma_{ijkl} = \gamma^{\mathrm{TP}}_{ijkl} + \gamma^{\mathrm{N}}_{ijkl}$, where γ^{TP} contains all the terms responsible for producing the maxima of absorption of two photons together with a few extra terms and γ^{N} contains what is usually called the negative component of γ. Accordingly

$$\gamma^{\mathrm{TP}}_{ijkl}(-\omega_\sigma;\omega_1,\omega_2,\omega_3) = K\frac{1}{\hbar^3}P(j,k,l;\omega_1,\omega_2,\omega_3)\sum_{o,p,q\neq f}\left\{\frac{\mu^i_{fo}\bar{\mu}^j_{op}\bar{\mu}^k_{pq}\mu^l_{qf}}{(\Omega_{of}-\omega_\sigma)(\Omega_{pf}-\omega_2-\omega_3)(\Omega_{qf}-\omega_3)} + \frac{\mu^j_{fo}\bar{\mu}^i_{op}\bar{\mu}^k_{pq}\mu^l_{qf}}{(\Omega^*_{of}+\omega_1)(\Omega_{pf}-\omega_2-\omega_3)(\Omega_{qf}-\omega_3)} + \frac{\mu^l_{fo}\bar{\mu}^k_{op}\bar{\mu}^i_{pq}\mu^j_{qf}}{(\Omega^*_{of}+\omega_3)(\Omega^*_{pf}+\omega_2+\omega_3)(\Omega_{qf}-\omega_1)} + \frac{\mu^l_{fo}\bar{\mu}^k_{op}\bar{\mu}^j_{pq}\mu^i_{qf}}{(\Omega^*_{of}+\omega_3)(\Omega^*_{pf}+\omega_2+\omega_3)(\Omega^*_{qf}+\omega_\sigma)}\right\} \qquad (3)$$

$$\gamma^{\mathrm{N}}_{ijkl}(-\omega_\sigma;\omega_1,\omega_2,\omega_3) = -K\frac{1}{\hbar^3}P(j,k,l;\omega_1,\omega_2,\omega_3)\sum_{o,q\neq f}\left\{\frac{\mu^i_{fo}\mu^j_{of}\mu^k_{fq}\mu^l_{qf}}{(\Omega_{of}-\omega_\sigma)(\Omega_{of}-\omega_1)(\Omega_{qf}-\omega_3)} + \frac{\mu^i_{fo}\mu^j_{of}\mu^k_{fq}\mu^l_{qf}}{(\Omega_{of}-\omega_1)(\Omega^*_{qf}+\omega_2)(\Omega_{qf}-\omega_3)} + \frac{\mu^j_{fo}\mu^i_{of}\mu^l_{fq}\mu^k_{qf}}{(\Omega^*_{of}+\omega_\sigma)(\Omega^*_{of}+\omega_1)(\Omega^*_{qf}+\omega_3)} + \frac{\mu^j_{fo}\mu^i_{of}\mu^l_{fq}\mu^k_{qf}}{(\Omega^*_{of}+\omega_1)(\Omega_{qf}-\omega_2)(\Omega^*_{qf}+\omega_3)}\right\} \qquad (4)$$

where $\omega_\sigma = \omega_1 + \omega_2 + \omega_3$ is the resulting frequency, f is the ground state, and o, p, and q are excited states. $P(j,k,l;\omega_1,\omega_2,\omega_3)$ is a permutation operator where each permutation of the Cartesian indexes (j,k,l) is associated with an equivalent permutation of the incident frequencies $(\omega_1,\omega_2,\omega_3)$. The transition dipole moment in the direction i, between states o and p, is given by μ^i_{op}, and $\bar{\mu}^i_{op} = \mu^i_{op} - \mu^i_{ff}\delta_{op}$ is the difference between the permanent dipole moments of states o and f. In the equation above, Ω_{of} is given by $\Omega_{of} = \omega_{of} - i\Gamma_o$, where $E_{of} = \hbar\omega_{of}$ is the transition energy between states f and o and Γ_o is the damping factor for the excited state o. In our calculations, we assumed the same value of $\hbar\Gamma = 0.1$ eV for all excited states. Using the perturbative definition of the hyperpolarizabilities,[63] the constant K in eqs 3 and 4 is equal to one-sixth.

In order to prepare eqs 3 and 4 for calculation of $\delta(\omega)$, we first need to apply the operator $P(j,k,l;\omega_1,\omega_2,\omega_3)$ to obtain 24 terms in each one and then replace $(-\omega_\sigma,\omega_1,\omega_2,\omega_3)$ by $(-\omega,\omega,\omega,-\omega)$ in the resulting equations.

In the procedure we advance in this article, instead of keeping all 24 terms of γ^{TP} we chose to retain only the four terms responsible for the two-photon absorption maxima, which yields results that are nearly identical to the ones obtained using all 24 terms, provided the incident photon frequency ω is far from the one-photon resonances ω_{of} or ω_{qf}. Equation 3, truncated to four terms, can then be simplified to

$$F = (\overline{\mu}^k_{pq}\mu^j_{qf} + \overline{\mu}^j_{pq}\mu^k_{qf})\,((\omega - i\Gamma - \omega_{of})\overline{\mu}^l_{op}\mu^i_{fo} + (\omega + i\Gamma - \omega_{of})\,\overline{\mu}^i_{op}\mu^l_{fo})$$

$$\gamma^{TP}_{ijkl} = \frac{1}{6\hbar^3}\sum_{o,p,q\neq f}\left(\frac{F}{(\Gamma^2 + (\omega - \omega_{of})^2)(\Gamma - 2i\omega + i\omega_{pf})(\Gamma - i\omega + i\omega_{qf})}\right) \quad (5)$$

We thoroughly tested the truncated version of γ^{TP} and found that, far from the one-photon resonances, it produces results that are nearly identical to the nontruncated equation at a lesser computational time. The 24 terms of γ^{N} can be factored into the following simpler and more compact form, containing only two different denominators, which we used in our calculations of $\delta(\omega)$

$$G = \omega_{of}(\Gamma^2 - \omega^2 + \omega^2_{of})((\Gamma - i\omega)^2 - \omega^2_{qf}) + \omega_{of}(\Gamma^2 + \omega^2 + \omega^2_{of})((\Gamma^2 + \omega^2) - \omega^2_{of})$$

$$\gamma^{N}_{ijkl} = \frac{1}{6\hbar^3}\sum_{o,q\neq f}\mu^i_{fo}\left(\frac{4(\Gamma^2 + \omega^2 - \omega^2_{of})(\omega_{of} + \omega_{qf})\mu^l_{fo}\mu^j_{fq}\mu^k_{fq}}{((\Gamma^2 + \omega^2)^2 + 2(\Gamma^2 - \omega^2)\omega^2_{of} + \omega^4_{of})((\Gamma - i\omega)^2 + \omega^2_{qf})} + \frac{4G(\mu^k_{fo}\mu^j_{fq} + \mu^j_{fo}\mu^k_{fq})\mu^i_{fq}}{((\Gamma^2 + \omega^2)^2 + 2(\Gamma^2 - \omega^2)\omega^2_{qf} + \omega^4_{qf})((\Gamma - i\omega)^2 + \omega^2_{of})^2}\right) \quad (6)$$

From eqs 5 and 6, it is also possible to show that $\gamma_{ijij} = \gamma_{iijj}$, further simplifying the calculation of $\langle\gamma\rangle$ in eq 2. The imaginary parts of eqs 5 and 6 are what we implemented in our procedure to calculate $\delta(\omega)$.

A common approximation employed in the interpretation of two-photon absorption spectra of linear quadrupolar molecules is the reduction of the system to only three levels. This approximation can be easily obtained from eq 5 by first assuming that the molecule is linear and therefore that the transition dipoles are aligned in the same direction, requiring us to calculate only the γ_{xxxx} component of the hyperpolarizability. Further, when the spectrum of absorption of one photon is dominated by a single transition $f \rightarrow o$, then $q = o$ in eq 5. In the notation of eq 5, the state that absorbs two photons is given by the index p and the frequency of the two absorbed photons is given by $\omega^{TP} = \omega_{pf}/2$. Because we want to calculate δ_{max}, the value of $\delta(\omega)$ in the maximum of the peak of absorption of two photons, we first make the substitution $\omega = \omega^{TP}$ in eq 5. When we solve the resulting equation for $\mathrm{Im}\gamma_{xxxx}$, we obtain an expression containing, in the denominator, the term $(4\Gamma^2 + (2\omega_{of} - \omega_{pf})^2)$. Assuming that $4\Gamma^2 \ll (2\omega_{of} - \omega_{pf})^2$, an approximation that is valid when we are not close to the double resonance condition $\omega_{of} = \omega_{pf}/2$ we can ignore the term in Γ^2 and finally obtain the expression for the three-level approximation

$$\mathrm{Im}\gamma^{3L}_{xxxx} = \frac{8}{3\hbar^3}\frac{(\mu^x_{fo}\mu^x_{op})^2}{\Gamma(2\omega_{of} - \omega_{pf})^2} = \frac{8}{3}\frac{(\mu^x_{fo}\mu^x_{op})^2}{\hbar\Gamma(2E_{of} - E_{pf})^2} \quad (7)$$

Equation 7 may be used with eq 2, which, within the linear molecule assumption, leads to $\langle\gamma\rangle = (1/5)\ \mathrm{Im}\ \gamma^{3L}_{xxxx}$, and subsequently, with eq 1 at the maximum absorption position $\omega^{TP} = \omega_{pf}/2$ in order to obtain an approximate three-level value for the cross-section, δ^{3L}. Equation 7 shows that in order to maximize $\delta(\omega)$ we need to either increase the values of the transition dipole moments μ^x_{fo} and μ^x_{op} or decrease the value of the detuning factor $2E_{of} - E_{pf}$. When adjusting the detuning factor, we need to be careful and make sure that we stay away from the double-resonance condition because, otherwise, the one-photon absorption peaks may overshadow the two-photon absorption ones, rendering the three-level approximation no longer valid.

It is important to stress that the three-level approximation in eq 7 was obtained from eq 5, which was in turn obtained taking the perturbative definition of the hyperpolarizabilities.[63] In the literature there are versions of the three-level approximation that are different from the one given in eq 7. As an example, Rumi et al.[32] write the three-level approximation as

$$\mathrm{Im}\gamma^{3L}_{xxxx} = \frac{4}{5}\frac{(\mu^x_{fo}\mu^x_{op})^2}{\hbar\Gamma(E_{of} - \hbar\omega^{TP})^2} = \frac{16}{5}\frac{(\mu^x_{fo}\mu^x_{op})^2}{\hbar\Gamma(2E_{of} - E_{pf})^2} \quad (8)$$

Equations 7 and 8 differ only in the constant K in front of the SOS eqs 3 and 4, a difference which depends on the particular convention used. Nevertheless, used consistently, both versions behave likewise in relating the values of δ^{3L} to the values of the parameters μ^x_{fo}, μ^x_{op}, and $2E_{of} - E_{pf}$.

To show that the computational procedure being advanced here is valid, we need to show that it is capable of delivering accurate values for both the one-photon and two-photon wavelengths, where the respective absorptions occur (λ_{opa} and λ_{tpa}), as well as useful values for the maximum cross-section for absorption of two photons (δ_{max}). When the goal is the design of organic systems with large values of cross-

(51) Moura, G. L. C.; Simas, A. M.; Miller, J. *Chem. Phys. Lett.* **1996**, *257*, 639.
(52) Zhou, J. F.; Kuzyk, M. G.; Watkins, D. S. *Opt. Lett.* **2006**, *31*, 2891.
(53) Perez-Moreno, J.; Zhao, Y.; Clays, K.; Kuzyk, M. G. *Opt. Lett.* **2007**, *32*, 59.
(54) Silva, A. M. S.; da Rocha, G. B.; Menezes, P. H.; Miller, J.; Simas, A. M. *J. Brazilian Chem. Soc.* **2005**, *16*, 583.
(55) Bezerra, A. G.; Gomes, A. S. L.; Athayde, P. F.; da Rocha, G. B.; Miller, J.; Simas, A. M. *Chem. Phys. Lett.* **1999**, *309*, 421.
(56) de Araujo, C. B.; Gomes, A. S. L.; Borissevitch, I. E. *Mol. Cryst. Liq. Cryst.* **2002**, *374*, 357.
(57) de Araujo, C. B.; Gomes, A. S. L.; Borissevitch, I. E. *Mol. Cryst. Liq. Cryst.* **2002**, *378*, 113.
(58) Menezes, L. D.; de Araujo, C. B.; Alencar, M. A. R. C.; Athayde, P. F.; Miller, J.; Simas, A. M. *Chem. Phys. Lett.* **2001**, *347*, 163.
(59) Rakov, N.; de Araujo, C. B.; da Rocha, G. B.; Simas, A. M.; Athayde, P. A. F.; Miller, J. *Chem. Phys. Lett.* **2000**, *332*, 13.
(60) Rakov, N.; de Araujo, C. B.; Rocha, G. B.; Simas, A. M.; Athayde-Filho, P. A. F.; Miller, J. *Appl. Opt.* **2001**, *40*, 1389.
(61) Pilla, V.; de Araujo, C. B.; Lira, B. F.; Simas, A. M.; Miller, J.; Athayde, P. F. *Opt. Commun.* **2006**, *264*, 225.
(62) Orr, B. J.; Ward, J. F. *Mol. Phys.* **1971**, *20*, 513.
(63) Willetts, A.; Rice, J. E.; Burland, D. M.; Shelton, D. P. *J. Chem. Phys.* **1992**, *97*, 7590.

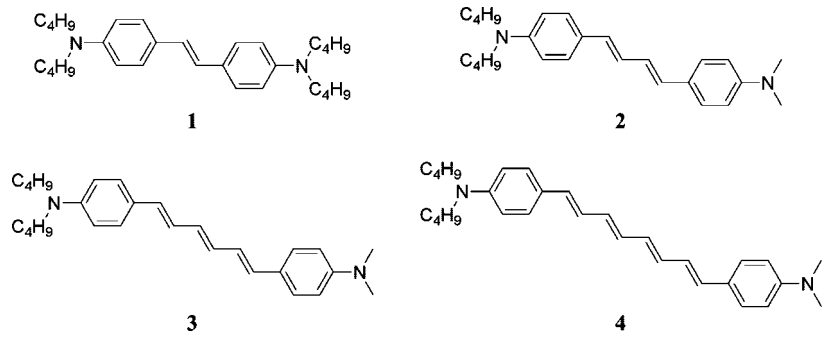

Figure 2. Homologous series of molecules selected to validate our computational procedure for the calculation of cross-sections for absorption of two photons, δ_{max}, for which there are δ_{max} and λ_{tpa} values obtained both experimentally and theoretically (using the MRD-CI technique by Rumi et al.[32]).

sections for absorption of two photons, exact values of δ_{max} are not needed. Within a homologous series it is enough for the computational procedure to be capable of ordering a set of compounds in terms of increasing values of δ_{max}. On the other hand, values of λ_{opa} and λ_{tpa} must be predicted with accuracy for the molecular designer to be able to guarantee that the two-photon absorption peak stays distant from the one-photon peak for the putative molecular structure under consideration.

In the next section, we show that our methodology is capable of producing values of λ_{opa}, λ_{tpa}, and δ_{max}, which are appropriate enough to perform the design of molecules for two-photon absorption applications.

3. Validation of the Computational Procedure

To obtain values of μ^i_{op} and E_{of} needed to calculate γ_{ijkl} using eqs 5 and 6, we performed configuration interaction (CI) calculations with the semiempirical INDO/S[64] Hamiltonian in the ZINDO program.[65] In order to obtain the molecular geometries necessary to do the CI calculations, we used the semiempirical AM1[66] Hamiltonian to optimize all the molecules.

To validate our computational approach, we followed the procedure by Rumi et al.,[32] where they selected a homologous series of four bis-donor diphenylpolyene molecules (see Figure 2) to have their δ_{max} and λ_{tpa} both calculated (using the multireference double CI method, MRD-CI) as well as determined experimentally by the two-photon-induced fluorescence method. In order to make the demanding MRD-CI calculations feasible, they replaced the original butyl groups in the actual synthesized molecules by methyl ones. In the present work, we performed our calculations for the same set of four molecules, which we call our validation set, but maintained their actual molecular structures with the butyl groups.

INDO/S has been parametrized to reproduce electronic spectra of molecules through configuration interaction with single excitations only, CIS. In principle, only INDO/S CIS calculations can be expected to yield electronic properties that can be compared with experiment. Indeed, semiempirical theory would predict that inclusion of double excitations in INDO/S would probably steer results away from the experimental values. On the other hand, in articles describing INDO/S calculations of δ_{max}, it is normal to include double excitations in the CI procedure either through CISD or MRD-CI. Thus, we decided to assess the impact of including double excitations in our procedure.

Table 1. Experimental (Rumi et al.[32]) and Theoretical INDO/S (CIS and CISD) Values of the Wavelengths, in nm, for the Maximum Absorption of One Photon (λ_{opa}) for the Molecules shown in Figure 2

			CISD	
molecule	experimental	CIS	108s+5d	50s+10d
1	374	358	281	246
2	390	379	288	240
3	412	400	301	249
4	430	416	314	242

As such, we performed three sets of CI calculations. For CIS, we requested an excitation window including up to 108 occupied and 95 unoccupied orbitals and included in the sum over states equation a total of 100 excited states and only searched for two-photon transitions with energies smaller than the energy of the first excited state, that is, the state that most strongly absorbs one photon. For the four molecules of the validation set, this requested excitation window includes all occupied and unoccupied orbitals. Indeed, molecule 1 of Figure 2, the largest of the four, possesses 88 occupied and 86 unoccupied orbitals only.

We further performed two sets of CISD calculations. In the first CISD set, we retained our single-excitation window, i.e., up to 108 occupied and 95 unoccupied molecular orbitals, and added to it all the double excitations that can be generated from a smaller window containing five occupied and five unoccupied molecular orbitals (we call this set CISD 108s+5d). In the second CISD set, we reduced the window of single excitations to only 50 occupied and 50 unoccupied molecular orbitals and increased the window of double excitations to 10 occupied and 10 unoccupied molecular orbitals (we call this set CISD 50s+10d).

The values of δ_{max} were obtained in the Göppert-Mayer unit, GM, which is equal to 10^{-50} cm^{4}s/photon.

In Table 1 we show a comparison between the INDO/S calculated wavelengths for the absorption of one photon (λ_{opa}) by CIS, CISD 108s+5d, and CISD 50s+10d and the experimentally determined values for our validation set. Not surprisingly, the CIS calculation was the one that performed best in comparison with experiment. When we add the double

(64) Ridley, J.; Zerner, M. *Theor. Chim. Acta* **1973**, *32*, 111.
(65) Zerner, M. C. *ZINDO Package, Quantum Theory Project*; University of Florida, Gainesville, FL, 1990.
(66) Dewar, M. J. S.; Zoebisch, E. G.; Healy, E. F.; Stewart, J. J. P. *J. Am. Chem. Soc.* **1985**, *107*, 3902.

Table 2. Experimental, Theoretical MRD-CI (Rumi et al.[32]), INDO/S CIS and CISD Values of the Maximum Wavelengths (in nm) for Absorption of Two Photons (λ_{tpa}) for the Molecules shown in Figure 2

				CISD	
molecule	experimental (ps data)	MRD-CI	CIS	108s+5d	50s+10d
1	605	484	495	341	357
2	640	519	523	356	352
3	695	544	548	369	364
4	695	564	569	381	365

Table 3. Experimental and Theoretical MRD-CI (Rumi et al.[32]), INDO/S CIS, and CISD Values of the Cross-Sections (in GM) for Absorption of Two Photons (δ_{max}) for the Molecules Shown in Figure 2 (1 GM = 10^{-50} cm^{4}s/photon)

				CISD	
molecule	experimental (ps data)	MRD-CI	CIS	108s+5d	50s+10d
1	240	147	355	384	138
2	230	195	603	577	295
3	340	219	938	885	538
4	410	227	1327	1698	701

excitations in the calculations, we observe a divergence between theory and experiment. Moving from a CISD 108s+5d to a CISD 50s+10d tends to unrealistically drive all four wavelengths to around 244 nm. When we add double excitations to the calculations there is a clear blue shift of the calculated wavelengths with errors that are as large as 100 nm for CISD 108s+5d.

In our cross-section calculations for the four molecules of the validation set we observed that for molecules 2, 3, and 4 our INDO/S CIS procedure predicts only one state that absorbs two photons with energy smaller than the energy for the one-photon transition. For molecule 1 it further predicts a very weak (δ_{max} = 8 GM) two-photon absorption at 571 nm. We dismissed this secondary absorption as being too weak. On the other hand, for the CISD 108s+5d technique, as many as five states that absorb two photons appear with energies smaller than the energy for the one-photon transition. Some of these transitions have very sizable cross-sections whose reality is to be questioned. We then selected the strongest transition for each of the molecules. For the CISD 50s+10d technique we found an unrealistic situation of as many as eight states absorbing two photons.

In Table 2 we show experimentally determined wavelengths for the maximum absorption of two photons (λ_{tpa}) (picosecond values) as well as their calculated values from CIS, MRD-CI, CISD 108s+5d, and CISD 50s+10d. Unlike the procedure employed by Rumi et al.[32] we do not engage in any process of configuration selection in our calculations. Nevertheless, their MRD-CI wavelengths are very similar to our INDO/S CIS ones, and both sets compare equally well with experiment. However, when we include double excitations in our calculations, results start to diverge from the experimental ones with a strong hypsochromic shift as can be clearly seen from Table 2. Moreover, moving from CISD 108s+5d to CISD 50s+10d, once again, tends to unrealistically squeeze the four wavelengths to a shorter interval centered at 360 nm, which is only 13 nm wide and 300 nm far from the experimental values.

For practical purposes, it is important to be able to more exactly predict the one- and two-photon absorption wavelengths for a putative molecule in order to ensure that both wavelengths stay away from each other. Otherwise, the one-photon absorption will dominate the events, compromising the practical usefulness of the molecule.

In Table 3, we show a comparison between the calculated maxima of the cross-sections for the absorption of two photons (δ_{max}) by CIS, MRD-CI, CISD 108s+5d, and CISD 50s+10d and the experimentally determined values from picosecond laser pulses. First, we observed that our calculations have a general tendency to overestimate the calculated cross-sections when compared to experiment (the only exception is the case of molecule 1 for the CISD 50s+10d calculation), whereas the MRD-CI calculations of Rumi et al.[32] underestimate δ_{max}.

If we restrict ourselves only to comparisons between calculated δ_{max}, we would reach the misleading conclusion that the CISD 50s+10d technique is the appropriate methodology to calculate the cross-sections for the absorptions of two photons. However, as already shown in Tables 1 and 2, the CISD 50s+10d technique is the one that produces the worst and somewhat wrong results for the absorption wavelengths. When we compare the calculated cross-sections for the CIS and CISD 108s+5d techniques, we can clearly observe that the results are not that much different from each other. Therefore, when the issue is the quality of the calculated cross-section results, our CIS technique performs similarly to the CISD 108s+5d technique. In addition, given the fact that the absorption wavelengths calculated by the CISD 108s+5d technique display an excessive hypsochromic shift when compared to experiment, INDO/S CIS then appears to be satisfactory.

This CISD observed hypsochromic shifts in the absorption wavelengths can be easily rationalized when we remember that the INDO/S Hamiltonian was parametrized to work with CIS only. When we add double or higher excitations in the calculations, overcorrelation appears in the ground state.

The results above serve as strong evidence that inclusion of double excitations in the INDO/S CI calculations unbalances the computational results. Not only does the number of excited absorbing states become unrealistically too large but also the calculated absorption wavelengths diverge from the experimental measurements. Because of the unreliable results produced by the INDO/S CISD approaches, from now on we will restrict our analyses to the INDO/S CIS methodology.

In Figure 3, we present graphical comparisons between the experimental values of λ_{tpa} for the homologous series in Figure 2 and the calculated ones by both the INDO/S CIS method being advanced in this article (Figure 3 top) and MRD-CI of Rumi et al.[32] (Figure 3 bottom). Clearly, there are very good linear correlations between the calculated and the experimental values. In Figure 4, we give graphical comparisons between the calculated and the experimental values of δ_{max} for the homologous series in Figure 2. We can observe that our INDO/S CIS values of δ_{max} show a better linear correlation with the experimental values than the MRD-CI ones calculated by Rumi et al.[32] Indeed, ordering of values is more important than obtaining the actual

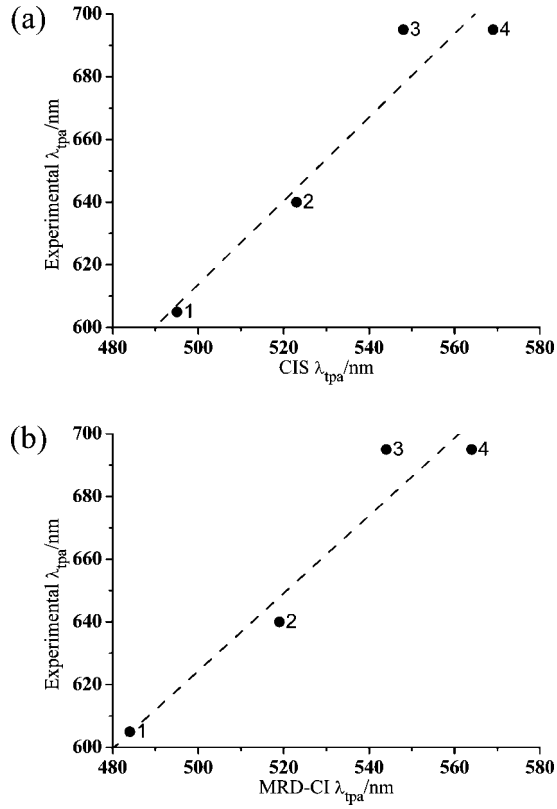

Figure 3. Experimental and calculated values of λ_{tpa} (in nm) for the molecules shown in Figure 2 for (a) our INDO/S CIS procedure and (b) the MRD-CI procedure of Rumi et al.[32]

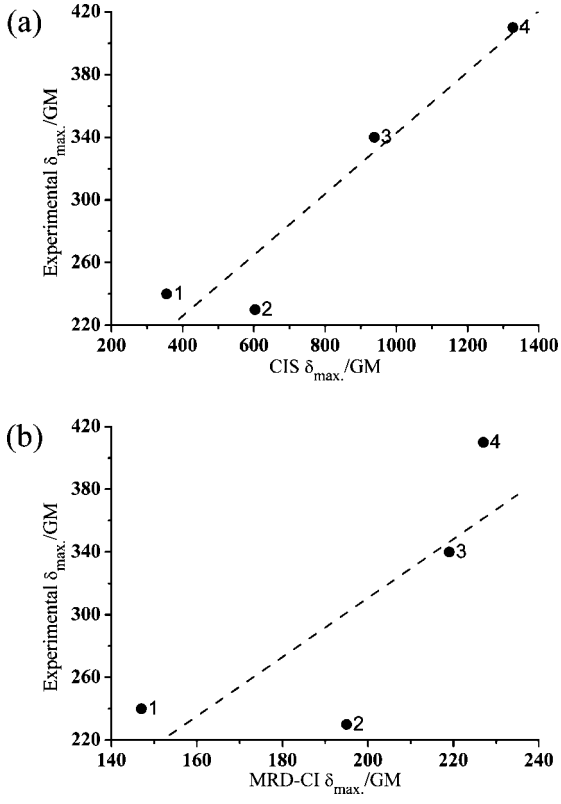

Figure 4. Experimental and calculated values of δ_{max} (in GM) for the molecules shown in 2 for (a) our INDO/S CIS procedure and (b) the MRD-CI procedure of Rumi et al.[32]

values when the interest is molecular design with the intent of generating putative structures.

Our approach can be further justified by what Guo et al.[67] found when they calculated the cross- sections for the absorption of two photons using both ab initio Hartree−Fock and density functional (DFT) methods. They detected that although inclusion of electron correlation through DFT can drastically increase the values of the calculated cross-sections, it has negligible effects on the relative ordering of the cross-sections for the molecules. In the conclusions section of their article, Guo et al. state very clearly that "Electron correlation is found to be very important for the absolute values of the TPA cross-sections, but not for the relative order of the TPA activity of the molecules under investigation." This statement adds to the justification of our methodology, which merely aims at ordering the molecules of interest in such a way as to guide selection of the most promising ones to be synthesized.

Our INDO/S CIS computational methodology ideally requires that all occupied and unoccupied orbitals be included in the requested excitation window. However, at present we have a machine limitation and are only able to request an excitation window with a maximum close to 108 occupied and 95 unoccupied orbitals in any given INDO/S CIS calculation. Of all 288 molecules that will be studied in the next section, 285 possess less than 108 occupied and 95 unoccupied orbitals. For these, the requested excitation window of up to 108 occupied and 95 unoccupied orbitals encompasses all available orbitals. For the remaining 3 larger molecules, we need to verify that the requested excitation window of 108 occupied and 95 unoccupied orbitals is enough to produce a converged enough value for the properties λ_{opa}, λ_{tpa}, and δ_{max} that can be useful for molecular design. Accordingly, as test cases we considered the three largest molecules of the next section, which we call $\mathbf{M_1}$, $\mathbf{M_2}$, and $\mathbf{M_3}$ and present in Figure 6. Figure shows the variation of the calculated wavelengths (in nm) for the absorption of one (λ_{opa}) and two photons (λ_{tpa}) as a function N_{CIS}, the maximum number of both occupied and unoccupied orbitals in the requested excitation window, employed in the CIS calculations. Indeed, the values of both λ_{opa} and λ_{tpa} increase with increasing N_{CIS} but show stability around $N_{CIS} \approx 108$. Moreover, Figure 7 shows graphs of the ratio $\delta_{max}/\delta_{max}[108]$ as function of N_{CIS} for molecules of Figure 5, where $\delta_{max}[108]$ is the value of δ_{max} for a fixed $N_{CIS} = 108$. Both graphs indicate that although a value of $N_{CIS} = 108$ is seemingly enough for even the largest molecules (with 113 occupied orbitals) considered in the next section, much smaller excitation windows (e.g., $N_{CIS} = 15$) would be clearly insufficient to yield converged values for these properties.

We can therefore conjecture that our INDO/S CIS computational methodology is appropriate for the design of compounds with large cross-sections for absorption of two photons based on calculations on homologous series of molecules.

(67) Guo, J. D.; Wang, C. K.; Luo, Y.; Agren, H. *Phys. Chem. Chem. Phys.* **2003**, *5*, 3869.

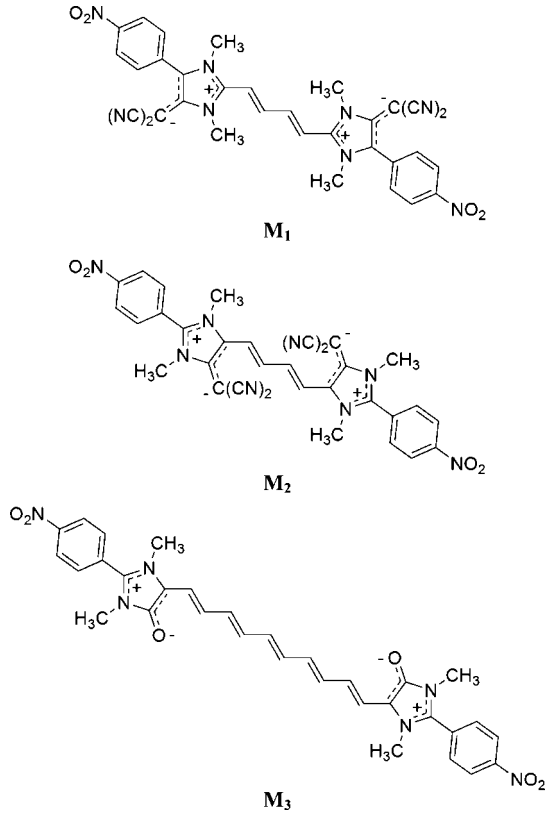

Figure 5. Structures of the three molecules of this article that possess the largest number of orbitals. We employed these molecules to study the behavior of the one- and two-photon absorption parameters (λ_{opa}, λ_{tpa}, and δ_{max}) as a function of the requested excitation window employed in the CIS calculations.

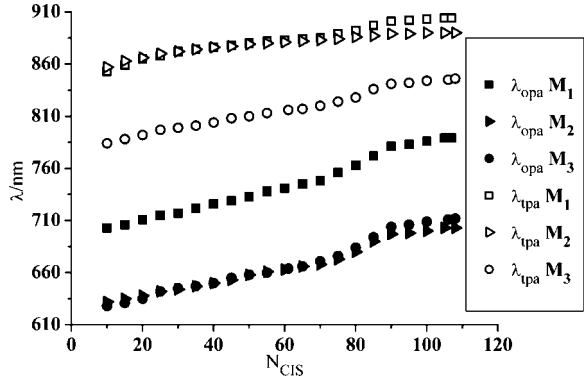

Figure 6. Variation of the calculated wavelengths (in nm) for absorption of one (λ_{opa}) and two photons (λ_{tpa}) as a function of N_{CIS}, the maximum number of both occupied and unoccupied orbitals in the requested excitation window employed in the CIS calculations, for the molecules shown in Figure 5. The squares are for molecule $\mathbf{M_1}$, the triangles for molecule $\mathbf{M_2}$, and the circles for molecule $\mathbf{M_3}$. The solid symbols are for λ_{opa} and the open symbols for λ_{tpa}.

4. Results and Discussion

As mentioned in the Introduction, the most commonly used molecular arrangements for two-photon absorption applications are linear quadrupolar arrangements. In our studies, we chose to apply this strategy by connecting two identical mesoionic rings through polyenic bridges. In Figure 8, we have two types of such structures. We can consider the anionic section of the mesoionic ring an electron-donor one, *D*, and the cationic section an electron acceptor, *A*. Structures where the mesoionic ring is linked to the polyenic bridge,

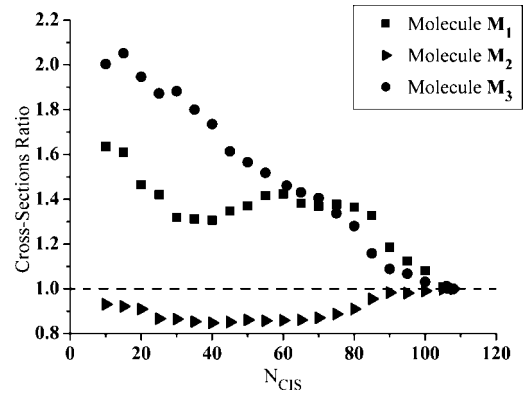

Figure 7. Graph of the ratios $\delta_{max}/\delta_{max}[108]$ as functions of N_{CIS} for the molecules shown in Figure 5. N_{CIS} is the maximum number of both occupied and unoccupied orbitals in the requested excitation window employed in the CIS calculations, and $\delta_{max}[108]$ is the value of δ_{max} for a fixed value of $N_{CIS} = 108$. The squares are for molecule $\mathbf{M_1}$, the triangles for molecule $\mathbf{M_2}$, and the circles for molecule $\mathbf{M_3}$.

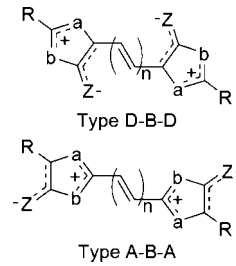

Figure 8. Two types of quadrupolar arrangements of two identical mesoionic rings connected through a polyenic bridge studied in this work: (a) donor−bridge−donor, represented by *D*−*B*−*D*, and (b) acceptor−bridge−acceptor, represented by *A*−*B*−*A*.

B, through the anionic section are labeled in this article as *D*−*B*−*D*, and structures where this linkage is through the cationic section are labeled as *A*−*B*−*A*. As indicated in Figure 8, in both types of structures we have the freedom of varying the mesoionic ring (*a*,*b*,*Z*) and the length of the polyenic bridge (*n*) as well as attaching extra (*R*) donor or acceptor groups to the system. As a result, we have the ability of generating molecules for calculations in a combinatorial manner. Accordingly, we allowed the number of systems being studied to be as large as we could accommodate, given our available computational resources. We did so in order to provide chemists with promising subclasses of compounds to be considered as synthetic targets. In this work, positions *a* and *b* in Figure 8 are filled with either *O*, *S*, or NCH_3 groups. The exocyclic group *Z* is replaced by *O* (olates), *S* (thiolates), NCH_3 (aminides), or $C(CN)_2$ (methylides).

Our first combinatorial study for the systems in Figure 8 was to establish which donor or acceptor groups connected to the mesoionic ring in position R would result in the largest calculated values of δ_{max}. We chose three different groups to place in position R: *p*-amino-phenyl (*p*-NH_2-Ph), phenyl (Ph), and *p*-nitro-phenyl (*p*-NO_2-Ph). To perform this study, we fixed the length of the polyenic bridge as $n = 2$ (butadiene bridge) and allowed the mesoionic ring (*a*,*b*,*Z*) to vary freely (36 different mesoionic rings). We therefore performed calculations on 216 different molecules of the *A*−*B*−*A* and *D*−*B*−*D* types. In Table 4 we present the average values of δ_{max} obtained for the six sets of 36 molecules (for each of

Table 4. Average Values of δ_{max} (in GM) Obtained for the Systems with Structures of Types $D-B-D$ and $A-B-A$ for Each of the Groups R Connected to the Various Mesoionic Rings Considered, for $n = 2$ (see Figure 8); Each Value Represents an Average of δ_{max} for 36 Molecules

	linkage type	
R	$D-B-D$	$A-B-A$
p-NH_2-Ph	655	1464
Ph	702	1245
p-NO_2-Ph	939	1072

Table 5. Average Values of δ_{max} (in GM) Obtained for the Systems with Structures of Types $D-B-D$ and $A-B-A$, Possessing Their Optimum Combination of Groups *R*, for Each of the Exocyclic Groups (Z) of the Various Mesoionic Rings for $n = 2$ (see Figure 8); Each Value Represents an Average of δ_{max} for 9 Molecules

	Z			
R	O	S	NCH_3	$C(CN)_2$
	linkage type $D-B-D$			
p-NO_2-Ph	1108	952	1065	632
	linkage type $A-B-A$			
p-NH_2-Ph	1831	1154	1727	1143

the R groups, for the two types of linkage of the mesoionic rings to the bridge, $A-B-A$ and $D-B-D$). First, we can observe in Table 4 that compounds with the $A-B-A$ arrangement have average values of δ_{max} larger than compounds with the $D-B-D$ arrangement. In other words, when we connect the mesoionic rings to the bridge through the cationic region we obtain values of δ_{max} that are, on average, larger than if we connect the mesoionic rings through the anionic region. This result is consistent with the proposal of Fujita et al.[40,41] in that introduction of cationic defects in the bridge produces values of δ_{max} that are larger than the ones obtained with introduction of anionic defects. In the case of the arrangement $A-B-A$ the connection of the donor group *p*-NH_2-Ph in the anionic region of the mesoionic ring was the one that resulted in the largest average value of δ_{max}. The acceptor group *p*-NO_2-Ph connected to the cationic region of the mesoionic ring was the combination that produced the largest average value of δ_{max} for systems with the arrangement $D-B-D$. It is worth accentuating that these two arrangements (*p*-NO_2-Ph for $D-B-D$ and *p*-NH_2-Ph for $A-B-A$) respect the natural polarization of the mesoionic rings.

Restricting ourselves only to molecules possessing the optimum combination of groups *R*, i.e., *p*-NO_2-Ph for type $D-B-D$ and *p*-NH_2-Ph for type $A-B-A$ molecules, we show in Table 5 the average values of δ_{max} obtained for each of the four exocyclic groups Z of the mesoionic ring. We show that, for both linkage types, the olate (Z = O) systems have average values of δ_{max} that are larger than the ones obtained for the other three exocyclic groups studied.

Among the 216 distinct molecules calculated in our first combinatorial study, we would like to identify those that are most promising for synthesis and subsequent measurement of their two-photon absorption properties. The appropriate strategy to choose these molecules cannot be based solely on selecting the systems with the largest calculated values of δ_{max}. It is also very important to take into consideration the distance between the one- and two-photon absorption

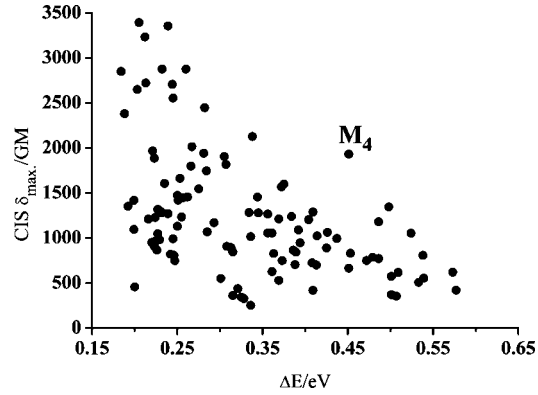

Figure 9. Calculated INDO/S CIS values of δ_{max} versus $\Delta E = E_{of} - E_{pf}/2$ for systems with the $A-B-A$ arrangement and $n = 2$ (see Figure 8). E_{of} and $E_{pf}/2$ are, respectively, the energies of the one- and two-photon transitions. This graph shows results for 108 distinct molecules, as defined by our combinatorial approach to molecular design.

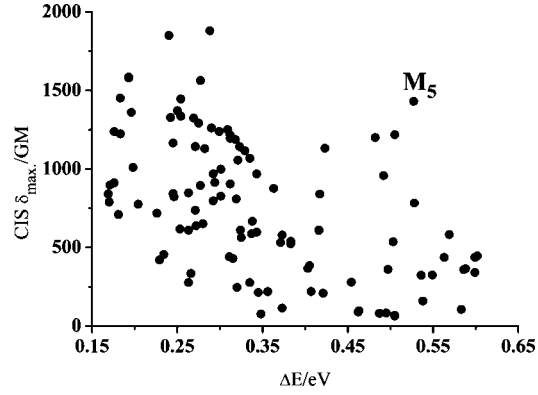

Figure 10. Calculated INDO/S CIS values of δ_{max} versus $\Delta E = E_{of} - E_{pf}/2$ for systems with the $D-B-D$ arrangement and $n = 2$ (see Figure 8). E_{of} and $E_{pf}/2$ are, respectively, the energies of the one- and two-photon transitions. This graph shows results for 108 distinct molecules, as defined by our combinatorial approach to molecular design.

peaks given by $\Delta E = E_{of} - E_{pf}/2$, where $E_{of} = hc\lambda_{opa}^{-1}$ and $E_{pf}/2 = hc\lambda_{tpa}^{-1}$. This distance is very important for practical purposes because we do not want these two peaks to get too close to each other; otherwise, the usually much larger single-photon absorption would impair the usefulness of the molecule for two-photon absorption applications.

In Figures 9 and 10 we show the graphs of δ_{max} versus ΔE for systems with $A-B-A$ and $D-B-D$ arrangements, respectively. We observe that several of the systems that have elevated values of δ_{max} also have small values of ΔE. In order to achieve the best compromise between having a large value of δ_{max} and also a value of ΔE that is not too small, we chose, as the most promising molecules for synthesis, the two molecules marked **M4** and **M5** in Figures 9 and 10, respectively. In Figure 11 we present the structures of these molecules along with their one-photon and two-photon absorption parameters. We observe that, based on our selection strategy, the most interesting molecules to be synthesized are both of the type 1,3-dioxolium-4-olate (a = O, b = O, and Z = O). In accordance with what would be expected based on the results from Table 4, in the case of the arrangement $A-B-A$ the best molecule, called **M4** in Figure 9, has the substituent R = *p*-NH_2-Ph and in the case of the arrangement $D-B-D$ the best molecule, called **M5** in Figure 10, has R = *p*-NO_2-Ph.

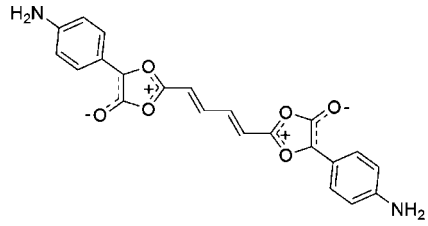

M₄

λ_{opa}=772nm λ_{tpa}=1073nm $\delta_{max.}$=1933GM

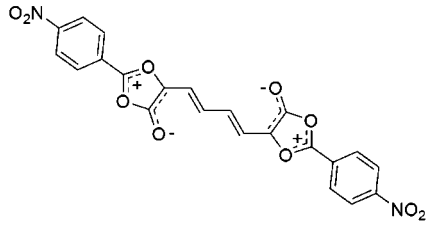

M₅

λ_{opa}=765nm λ_{tpa}=1134nm $\delta_{max.}$=1431GM

Figure 11. Structures of the most promising systems with the $A-B-A$ (**M₄**) and $D-B-D$ (**M₅**) arrangements with $n = 2$ (see Figure 8). Their values of λ_{opa}, λ_{tpa}, and δ_{max} are also shown.

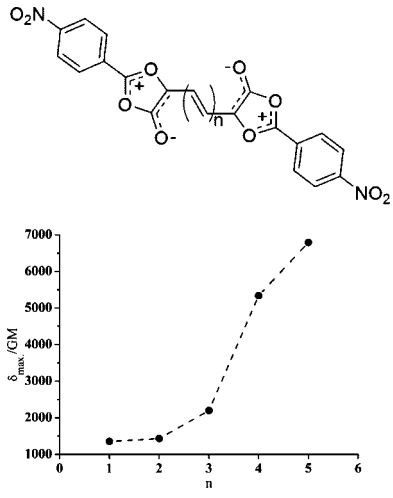

Figure 12. Example of a typical curve of δ_{max} (INDO/S CIS calculated) versus n for a system with the arrangement $D-B-D$ with R = p-NO_2-phenyl (see Figure 8). The mesoionic ring used was the (O,O,O). The dashed lines are present just to guide the eye.

As we have seen in Tables 1 and 2, the INDO/S CIS calculations predict with relative accuracy the energy of the one-photon transition (E_{of}) while overestimating the energy of the state that absorbs two photons (E_{pf}). The result is that the values of ΔE in Figures 9 and 10 are being underestimated. It is therefore expected that the experimental distance between the one- and two-photon absorption peaks will be favorably larger than the calculated values.

The last remaining parameter that we could vary in a combinatorial study, for the structures shown in Figure 8, is the length of the polyenic bridge (n). For this part of the study we restricted our attention only to molecules possessing the optimum combination of groups R, i.e., p-NO_2-Ph for type $D-B-D$ and p-NH_2-Ph for type $A-B-A$ molecules, and only to the olate (Z = O) systems. We chose to allow

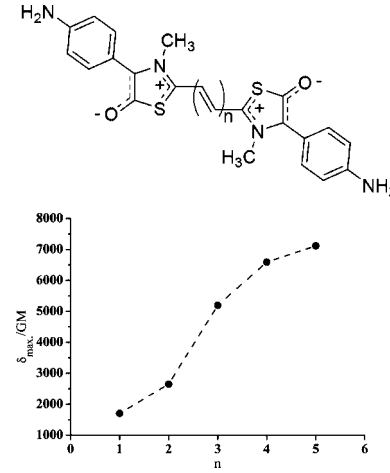

Figure 13. Example of a typical curve of δ_{max} (INDO/S CIS calculated) versus n for a system with the arrangement $A-B-A$ with R = p-NH_2-phenyl (see Figure 8). The mesoionic ring used was the (NCH_3,S,O). The dashed lines are present just to guide the eye.

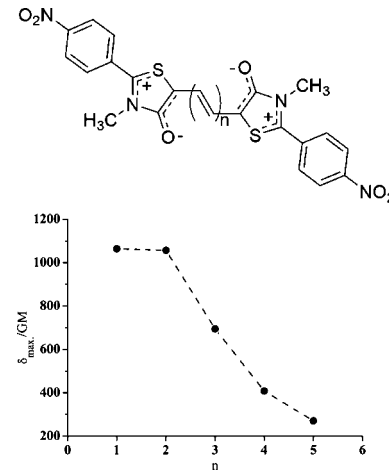

Figure 14. Example of a typical curve of δ_{max} (INDO/S CIS calculated) versus n for a system with the arrangement $D-B-D$ with R = p-NO_2-phenyl (see Figure 8). The mesoionic ring used was the (S,NCH_3,O). The dashed lines are present just to guide the eye.

the length of the polyenic bridge to vary from $n = 1$ to 5, and therefore, we had a series of 90 distinct molecules to study.

For the mesoionic rings that did not contain sulfur in position a of the ring, the curves of δ_{max} versus n display an overall upward trend, although not always strictly monotonic. For the cases where position a of the mesoionic ring is occupied by sulfur, we observed a decrease of δ_{max} with increasing length of the polyenic bridge. In some cases, this decrease is not monotonic, with the maximum value of δ_{max} for a given series located at $n = 2$ instead of $n = 1$. In Figures 12–15, we show some examples of typical curves of δ_{max} versus n.

In an attempt to explain these results we will interpret them using a three-level system rationale. In addition, in order to validate this rationale we will first apply it to the four bis-donor diphenylpolyene molecules shown in Figure 2. The experimental and our calculated INDO/S CIS values of δ_{max} for these four systems can be found in Table 3 and are compared in Figure 4a. In Table 6, we show the results obtained for these analyses of reduction to three levels.

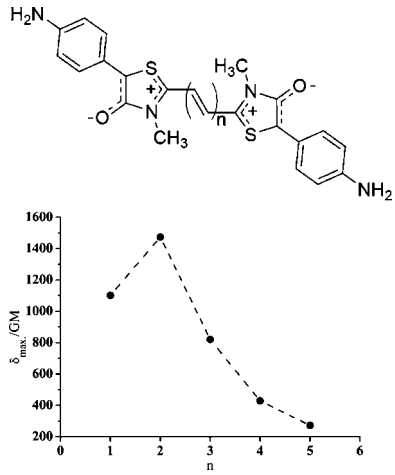

Figure 15. Example of a typical curve of δ_{max} (INDO/S CIS calculated) versus n for a system with the arrangement $A-B-A$ with R = p-NH_2-phenyl (see Figure 8). The mesoionic ring used was the (S,NCH_3,O). The dashed lines are present just to guide the eye.

Table 6. Three-Level Analysis for the Systems Shown in Figure 2[a]

n	E_{of}	E_{pf}	μ_{fo}	μ_{op}	$(2E_{of} - E_{pf})$	δ^{3L}	δ^{neg}	δ^{corr}
1	3.461	5.005	10.03	13.70	1.917	388	−5	383
2	3.267	4.744	11.78	15.16	1.790	675	−11	664
3	3.100	4.523	13.47	16.40	1.677	1070	−23	1047
4	2.976	4.359	14.99	17.44	1.593	1542	−39	1503

[a] The energies of the main excited states (E_{of} and E_{pf}) are in units of eV, the transition dipole moments (μ_{fo} and μ_{op}) are in units of Debye, and the cross-sections are in units of GM. See text for the definitions of the cross-sections δ^{3L}, δ^{neg}, and δ^{corr}.

Because the angles between the transition dipole moments μ_{fo} and μ_{op} were all smaller than 10°, we decided to use the norms of the vectors to calculate the approximate cross-sections instead of projecting one vector onto the direction of the other. The column labeled δ^{3L} in Table 6 contains δ_{max} from the three-level approximations for the cross-sections obtained using eq 7, together with eqs 1 and 2. We can observe in Table 6 that, even though the three-level approximation systematically overestimates the values of the cross-sections, there is good agreement between the values obtained using this approximation (δ^{3L}) and the values obtained using all the excited states in the sum (δ_{max}). In obtaining the three-level approximation we have to make the assumptions that (a) the molecule is linear, (b) the spectrum of absorption of one photon is dominated by a single transition, (c) $4\Gamma^2 \ll (2\omega_{of} - \omega_{pf})^2$, and (d) the negative contribution of γ is negligible (an assumption that is implicit when we take $4\Gamma^2 \ll (2\omega_{of} - \omega_{pf})^2$). Indeed, the molecules studied in Table 6 are all approximately linear, possess one dominant one-photon transition, and have $(2\omega_{of} - \omega_{pf})$ much greater than 2Γ. Consequently, as expected, the results obtained using the three-level approximation are comparable with the results obtained using the nonapproximated version of the SOS equations.

In Figure 16 we show graphs of the values of δ_{max} and δ^{3L} versus n for these molecules and observe an approximate linear increase of the cross-sections as function of n. In the three-level approximation we completely ignore the contribution of the negative component of the hyperpolarizability, γ^{N}, as well as all other excited states. We can include a semiexact correction due to the negative component of the

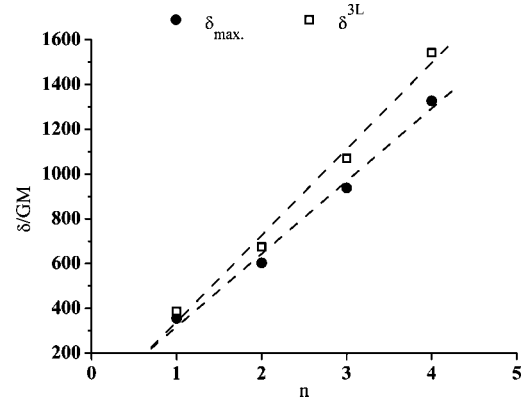

Figure 16. Cross-sections (in GM) versus n for the systems in Figure 2. The circles are for the cross-sections obtained using our INDO/S CIS procedure (δ_{max}), and the squares are for the cross-sections obtained by the three-level approximation (δ^{3L}).

hyperpolarizability to the three-level approximation using the same assumptions employed to obtain the three-level approximation, i.e., (i) $\omega = \omega^{TP}$, (ii) only the x component of the hyperpolarizability contributes, and (iii) only a single excited state o absorbs one photon. This correction is given by

$$C = 512\Gamma\omega_{of}\omega_{pf}\big(64(2\Gamma^2 - 3\omega_{of}^2)(\Gamma^2 + \omega_{of}^2)^2 + 16(3\Gamma^4 + 4\Gamma^2\omega_{of}^2 + 5\omega_{of}^4)\omega_{pf}^2 - (4\omega_{of}^2 + \omega_{pf}^2)\omega_{pf}^4\big)$$

$$\mathrm{Im}\gamma_{xxxx}^{neg} = \frac{1}{3\hbar^3}\frac{C}{\big(16(\Gamma^2 + \omega_{of}^2)^2 + 8(\Gamma^2 - \omega_{of}^2)\omega_{pf}^2 + \omega_{pf}^4\big)^3}(\mu_{fo}^x)^4 \quad (9)$$

The column labeled δ^{neg} in Table 6 contains the values of these negative corrections, obtained using eq 9 together with eqs 1 and 2. The column labeled δ^{corr} in Table 6 contains the final corrected values of the cross-sections given by $\delta^{corr} = \delta^{3L} + \delta^{neg}$. We observe in Table 6 that although the value of δ^{neg} is small for these molecules, after we add the negative corrections the values of δ^{corr} show a slightly improved agreement with δ_{max}. In Figure 17 we show the graphs of the values of δ^{neg} and δ^{corr} versus n, and also in this case there is an approximately linear relation between δ^{corr} and n. It is worth mentioning that the values of δ^{neg} versus n show a slightly parabolic behavior. The data in Table 6 show that for the molecules in Figure 2 the increase in the cross-sections, as the length of the polyenic bridge increases, is the result of an increase in the transition dipole moments (μ_{fo} and μ_{op}) combined with a decrease in the transition energies, producing a decrease in the detuning factor ($2E_{of} - E_{pf}$).

When we applied the three-level approximation analysis to the systems containing mesoionic rings, we found that, unlike the case of the molecules shown in Figure 2, which have only one excited state absorbing two photons in the region of energy we are studying, these molecules show two excited states, p and p', that absorb two photons. This simple fact is the key to explaining the unusual behavior observed for the quadrupolar systems containing mesoionic rings. In Table 7, we show the three-level approximation analysis for the ring (NCH_3,S,O) with the arrangement $A-B-A$ and R = p-NH_2-phenyl. The graph of δ_{max} versus n for this system

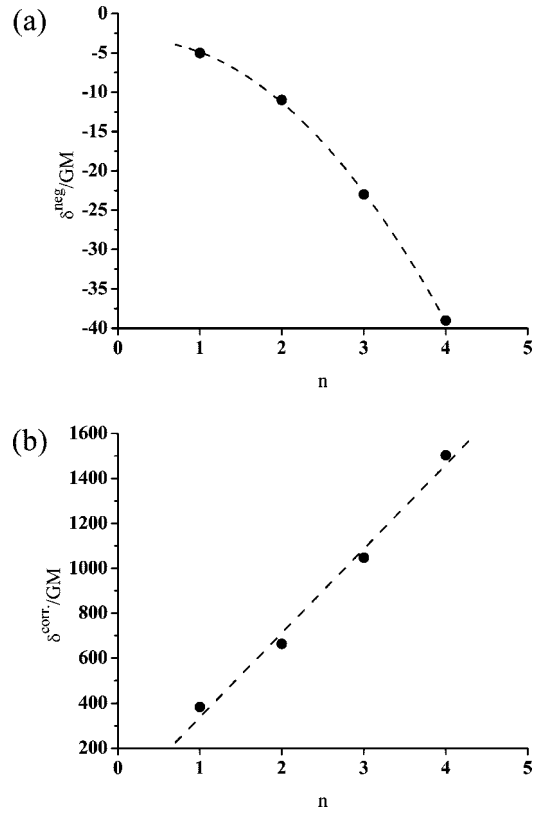

Figure 17. cross-sections (in GM) versus n for systems in Figure 2: (a) negative corrections to the three-level system (δ^{neg}) values, and (b) final corrected values of the cross-sections (δ^{corr}).

can be seen in Figure 13. In the graph the point for $n = 1$ represents the cross-section for absorption to the lower excited state p, and the other points are for excitation to the higher state p'. When only the excited state p is available for absorbing two photons, as is the case when the state p' is close to the double-resonance condition and falls under the domain of the negative contribution of the hyperpolarizability, the cross-section decreases as the length of the polyenic bridge increases. When the excited state p' is available for absorbing two photons, the cross-section increases as the polyenic bridge enlarges.

The three-level reduction analysis shows that as the length of the bridge increases, μ_{fo} increases, μ_{op} decreases and then nearly saturates, and $\mu_{op'}$ increases and then saturates. The detuning factor for the transition to the state p increases with the length of the polyene, and this together with the reduction of μ_{op} results in the decrease of the cross-section for two-photon absorption to this state. The detuning factor for the transition to the state p' is essentially constant for n between 2 and 5 (for $n = 1$ this transition is in the negative region of the cross-section), and the increase in the cross-section for two-photon absorption to this state is essentially due to the increase in the transition dipole moments. It is important to emphasize that for all the mesoionic rings studied there was not a single case where all the transitions occur only to state p'. The up−down behavior for δ_{max} versus n observed in Figures 12–15 is due to this simple fact. Another very important point that must be emphasized is the fact that a single three-level approximation (δ^{3L}) is not a very good approximation to δ_{max} for systems containing mesoionic rings. This is a direct consequence of the smaller values of the detuning factors observed in these molecules. The negative contribution to the cross-section (δ^{neg}) is large and the final corrected cross-section (δ^{corr}) is still not close to δ_{max}. Even though the three-level results are not numerically close to δ_{max}, in Figure 18 we show there is still a good linear correlation of δ_{max} with both δ^{3L} and δ^{corr}. The correlation between δ_{max} and δ^{corr} is slightly better than the one between δ_{max} and δ^{3L}.

We now employ our selection strategy to the 90 molecules of our second combinatorial study. In Figures 19 and 20 we have the graphs of δ_{max} versus ΔE for the systems with the $A-B-A$ and $D-B-D$ arrangements, respectively. In each of the graphs we have two molecules marked **M4** and **M6** in Figure 19 and **M5** and **M7** in Figure 20. The molecules **M4** and **M5** are the same ones marked in Figures 9 and 10 and shown in Figure 11. Molecules **M6** and **M7** were chosen as examples of systems that have large values of δ_{max} but values of ΔE that are small enough to render them uninteresting for synthesis. In Figure 21 we show the structures and one- and two-photon absorption parameters of molecules **M6** and **M7**.

It is worth saying that our results serve as an excellent basis to claim that linear quadrupolar arrangements of mesoionic rings connected through a polyenic bridge are good candidates for systems with high values for the cross-section for absorption of two photons.

Table 7. Three-Level Analysis for the Ring (NCH_3,S,O) with the Arrangement $A-B-A$ and R = p-NH_2-phenyl[a]

energies and transition dipoles								
N	E_{of}	E_{pf}	$E_{p'f}$	μ_{fo}	μ_{op}	$\mu_{op'}$	$(2E_{of} - E_{pf})$	$(2E_{of} - E_{p'f})$
1	1.471	2.490	2.651	17.34	12.87	6.66	0.452	0.291
2	1.514	2.355	2.656	18.19	8.05	14.90	0.673	0.372
3	1.572	2.223	2.761	18.90	6.52	17.04	0.921	0.383
4	1.627	2.125	2.870	19.60	6.05	17.68	1.129	0.384
5	1.671	2.055	2.967	20.29	5.85	17.67	1.287	0.375

absorption cross-sections								
N	δ^{p}_{max}	$\delta^{p'}_{max}$	δ^{3L}_{p}	$\delta^{3L}_{p'}$	δ^{neg}_{p}	$\delta^{neg}_{p'}$	δ^{corr}_{p}	$\delta^{corr}_{p'}$
1	1704		4554	3335	−2077	−7189	2477	−3854
2	479	2650	791	11284	−626	−4912	165	6372
3	136	5195	267	16242	−216	−5712	51	10530
4	69	6590	150	20212	−108	−7070	42	13142
5	44	7115	108	24247	−72	−9223	36	15024

[a] The energies of the excited states (E_{of}, E_{pf}, and $E_{p'f}$) are in units of eV, the transition dipole moments (μ_{fo}, μ_{op}, and $\mu_{op'}$) in units of Debye, and the cross-sections in units of GM. See text for the definitions of the cross-sections δ^{3L}, δ^{neg}, and δ^{corr}.

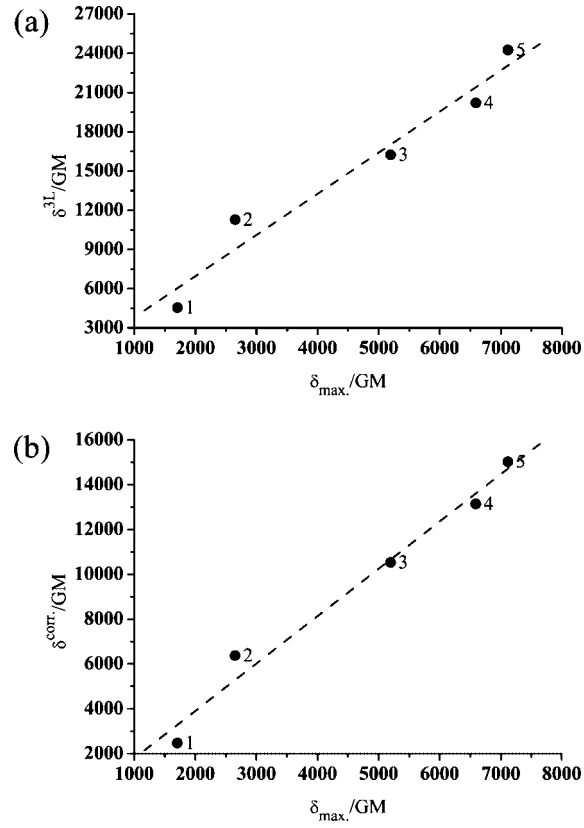

Figure 18. Comparison between the values of δ_{max} (in GM) calculated using our INDO/S CIS procedure and the values of (a) δ^{3L} and (b) δ^{corr}, obtained using the three-level analysis for compounds with the arrangement $A-B-A$ and ring (NCH_3,S,O); R = p-NH_2-phenyl (see Figure 13) and for various numbers of conjugated double bonds in the polyenic bridge (indicated by the numeral next to the respective circle points).

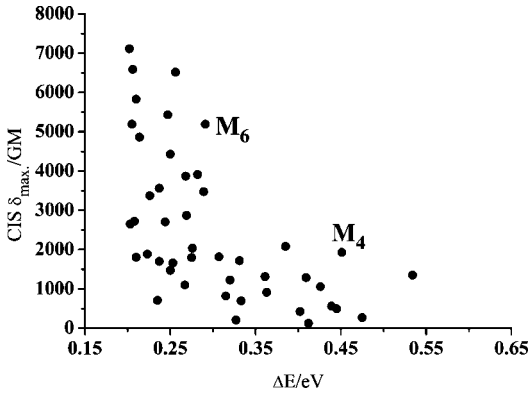

Figure 19. Calculated INDO/S CIS values of δ_{max} versus $\Delta E = E_{of} - E_{pf}/2$ for the systems with the $A-B-A$ arrangement with Z = O and R = p-NH_2-phenyl for n varying between 1 and 5 (see Figure 8). E_{of} and $E_{pf}/2$ are, respectively, the energies of the one- and two-photon transitions. This graph shows results for 45 distinct molecules, as defined by our combinatorial approach to molecular design.

5. Conclusions

In this article, we advance a computational procedure, based on INDO/S CIS semiempirical electronic structure method, much faster than MRD-CI ones, which allows us to calculate the parameters needed to describe the process of absorption of two photons by organic molecules. Further, we simplified the calculation by retaining only terms that contribute to the peaks of absorption of two photons and, for the first time, arrived at a much more compact form for

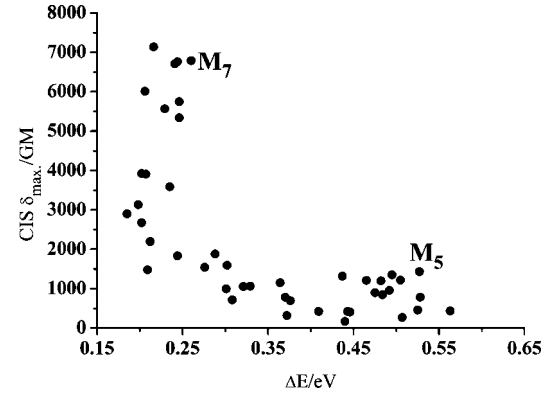

Figure 20. Calculated INDO/S CIS values of δ_{max} versus $\Delta E = E_{of} - E_{pf}/2$ for the systems with the $D-B-D$ arrangement with Z = O and R = p-NO_2-phenyl for n varying between 1 and 5 (see Figure 8). E_{of} and $E_{pf}/2$ are, respectively, the energies of the one- and two-photon transitions. This graph shows results for 45 distinct molecules, as defined by our combinatorial approach to molecular design.

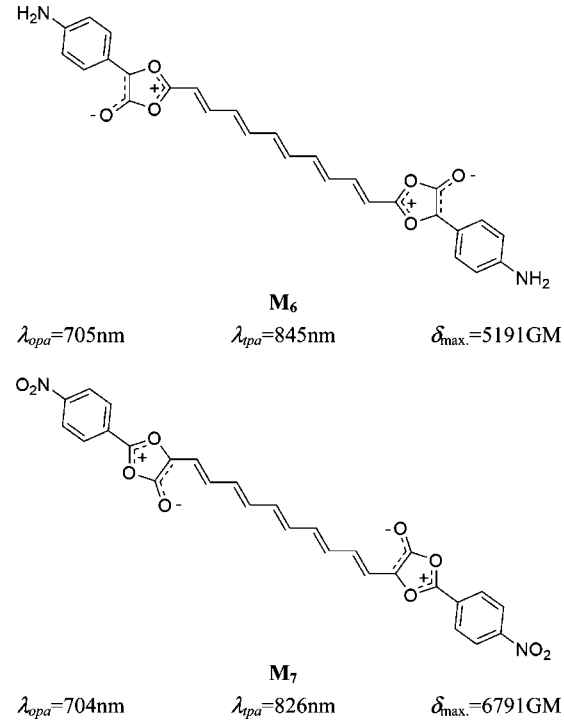

Figure 21. Structures of the systems with the $A-B-A$ ($\mathbf{M_6}$) and $D-B-D$ ($\mathbf{M_7}$) arrangements (see Figure 8) marked in Figures 19 and 20, respectively. Also identified are their values of λ_{opa}, λ_{tpa}, and δ_{max}.

the hyperpolarizability negative component. Furthermore, we show that when applied to a series of homologous compounds this procedure is capable of ordering the molecules in terms of increasing values of δ_{max} and also yields useful values for both λ_{opa} and λ_{tpa}.

We now have the necessary requirements to perform combinatorial molecular design of organic systems which can be expected to display large values of cross-sections for absorption of two photons, coupled with a sizable enough separation of one- and two-photon absorption peaks. Accordingly, we used the approach advanced here to obtain values of λ_{opa}, λ_{tpa}, and δ_{max} for organic compounds with quadrupolar arrangements of type A mesoionic rings. For the quadrupolar systems containing mesoionic rings we found that the largest calculated

average values of δ_{max} are obtained for molecules where the polyenic bridge is linked to the rings through their cationic region. This result is consistent with the proposal of Fujita et al.[40,41] in that introduction of cationic defects results in larger values of δ_{max}. When we made the polyenic bridge longer, we found that, in some cases, the values of δ_{max} decrease as n increases. This behavior was clarified using analysis based on reduction of the systems to three levels. Finally, we showed that quadrupolar organic molecules possessing mesoionic rings are good candidates for systems with large cross-sections for absorption of two photons. Syntheses of such systems are presently being attempted in our laboratories.

Acknowledgment. We acknowledge financial support from CNPq and CAPES (Brazilian agencies), the Instituto do Milênio de Materiais Complexos, and CENAPAD (Centro Nacional de Processamento de Alto Desempenho em São Paulo) for access to their computational facilities.

CM070369O